Interference of multiphoton light and its classical model

A. V. Belinskii and D. N. Klyshko

M. V. Lomonosov Moscow State University

(Submitted 20 May 1992)
Zh. Eksp. Teor. Fiz. **102**, 1116–1125 (October 1992)

On the basis of an analysis of the interference of different orders n, we have established that in low orders $n \leqslant 2$ the predictions of the classical and quantum theory can differ only quantitatively: Only the visibility of interference in the quantum case exceeds the classical visibility. The situation changes radically for $n \geqslant 3$: Significant qualitative differences between the classical and quantum interference structures appear; for example, for $n = 4$ the interference maximum appearing in the quantum description becomes a minimum in the classical description.

INTRODUCTION

Interest in different experiments on the observation of light interference ($n = 2$), performed, as a rule, in the photon-counting mode using parametric sources of two-photon radiation (see, for example, Refs. 1–5 and the review Ref. 6), has increased in the last few years. In these experiments, two-channel detection is used and only cases in which two photons appear simultaneously in the channels, the probability for which is proportional to the moment $G'_{11} = \langle n_a n_b \rangle$, where $n_j \equiv a_j^+ a_j$ is the photon number operator for the channel j and the prime refers to the output of the interferometer, are used in the calculations.

This interest is motivated by endeavors to observe purely quantum effects which do not have classical analogs. However, the interferometers employed are linear systems which cannot introduce into the experiment any specifically quantum features: The interferometers are adequately described classically and they are only linear transducers of the input moments of the radiation fed into them.[6–8] For $n = 2$, for example, G'_{11} is a linear combination of three moments G_{11}, $G_{20} \equiv \langle :n_a^2: \rangle$, and $G_{02} \equiv \langle :n_b^2: \rangle$ of the input radiation. If the starting beams are symmetric, then $G_{02} = G_{20}$. Thus the "quantumness" or classicality of the observed effects lies only in the relation between the two moments G_{11} and G_{02} at the input to the interferometer, whose relative values in the classical and quantum cases can differ very substantially.[6–8] As a result, the only manifestation of specifically quantum nature gives rise to a purely quantitative difference: an increase in the visibility V of the interference pattern as a result of the strong inequality $G_{11} \gg G_{02}$. We recall that by interference, in this case, we mean the dependence of the counting rate of coincidences of the photons recorded in the channels on the phase delay 2φ that is introduced. This dependence has the form

$$R_c(\varphi) \sim G_{11}'(\varphi) \sim 1 + V \cos 4\varphi \equiv f(\varphi).$$

By classical description we mean here a theory that employs Maxwell's equations with stochastic classical fields (the brackets $\langle ... \rangle$ denote an average weighted with some nonnegative distribution function of the field) and the semiclassical theory of the process of photoionization in the detectors. A more general classical description of the correlation of the photocounts, separated by space-like intervals, with the help of hidden variables $\{\lambda\}$ (see, for example, Refs. 9 and 10), is also of great interest. In this approach there exists a critical value of the visibility, values above which can be interpreted with the help of Bell's inequalities[11] as an indication of nonlocality and (or) nonpositiveness of the distribution function $P(\{\lambda\})$. These three approaches—quantum, stochastic, and hidden-variable—were recently compared by Su and Wodkeiwich.[12]

It should also be noted the degradation of the classical visibility $V_{\rm cl}$ when the finite triggering time of the detection system is taken into account can be quite dramatic; i.e., it results in virtually complete vanishing of interference within the limits of sensitivity of the measuring channel of the setup. But interference modulation itself is always present in both the classical and quantum descriptions.

A somewhat different situation obtains when multiphoton processes are used and when moments of higher orders are recorded instead of the interference of amplitudes or intensities ($n = 1,2$). The formation of G'_{KL} ($K + L \geqslant 3$) now involves a larger number of input moments G_{KL}, the observed consequences of whose superposition, remaining linear as before, can nonetheless manifest qualitative differences from the classical and quantum treatments. We discovered this possibility in an analysis of the two-mode interference of three- and four-photon states and it is the subject of the exposition given below. It is interesting that the analysis of the correlation of three or more photons also reveals a new type of contradiction between the quantum theory and the concept of hidden variables (see Refs. 9 and 10).

1. INTERFERENCE OF THREE-PHOTON STATES

The proposed experiment can be conducted in two equivalent modifications, illustrated in Fig. 1. Version *a* employs a Mach–Zehnder (M–Z) interferometer, while variant *b* employs its polarization version. There are no fundamental differences in the description of such systems,[6] but their actual implementation, of course, has definite specific features.

In both cases the following fundamental possibilities exist for preparing three-photon states $|21\rangle$, i.e., two photons in the mode a and one photon in the mode b. First, it is possible to use a three-stage transition of the atom from the excited state into the ground state, in which two of the three emitted photons are degenerate (they belong to the same mode). An alternative method is to use parametric scattering either in a medium with cubic nonlinearity $\chi^{(3)}$ (Ref. 13) or as a result of a cascade process, analogous to that described in Refs. 6 and 14. In the latter case, two photons are generated at the first stage in the course of nondegenerate parametric scattering in a piezoelectric crystal, for example,

 0038-5646/92/100606-05$05.00

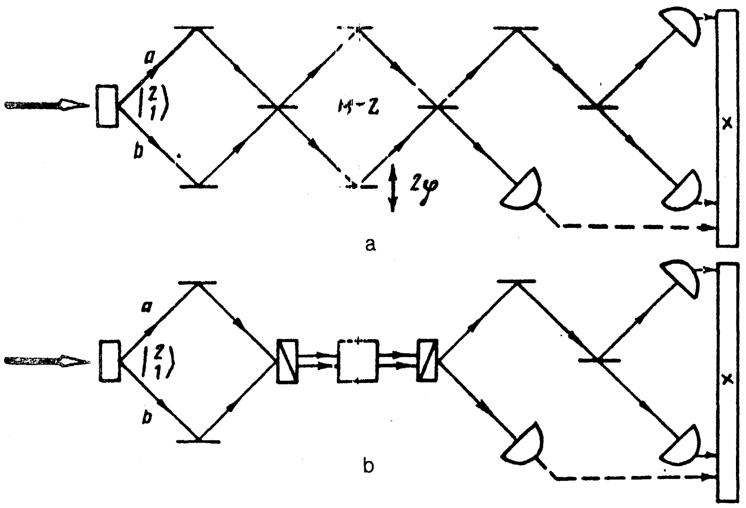

FIG. 1. Possible variants of schemes for observing two-mode three-photon interference: a) two-arm Mach–Zehnder (M–Z) interferometer; b) polarization type interferometer. F is a Faraday rotator of the polarization plane. All beam splitters have the same (50%) transmission and reflection. The coincidence scheme fixes only the cases of simultaneous detection of a photon by each of the three photodetectors.

of the type $3\omega \to 2\omega + \omega$, while in the second case splitting of one of these photons in a degenerate parametric process is used, i.e., generation of the subharmonic $2\omega \to \omega$.

The modes a and b formed in this manner are then fed into the interferometer. Of course, the modes must have the same carrier frequencies and in the polarization variant they must differ only by the polarization state. The phase delay in one arm of the M–Z interferometer can be controlled by displacing one of the mirrors (see Fig. 1a), while in the polarization interferometer it can be controlled with the help of a rotator of the Faraday (F) rotator type (Fig. 1b).

The output beams are recorded with photodetectors, the signals from which are processed by a coincidence system and averaged, and as a result the required moment G'_{KL} is calculated. For example, in order to measure G'_{21} it is convenient to use three photodetectors, as shown in Fig. 1.

The four-photon process of formation of a three-photon state, which consists of a decay of one pumping photon into three photons, is described by the following Hamiltonian:

$$H_3 = i\hbar\chi (a^{+2}b^{+} - a^2 b)/2^{1/2}, \tag{1.1}$$

where a and b are operators which annihilate a photon of the corresponding modes, a^+ and b^+ are creation operators, and the coefficient χ characterizes the nonlinearity of the system (when parametric scattering in a medium with cubic nonlinearity is employed, χ is proportional to $\chi^{(3)}$ and to the pump amplitude; the pumping is assumed to be classical and inexhaustible).

In the Heisenberg representation the evolution of the operators is determined by the following equations of motion:

$$da/d\tau = 2^{1/2} a^+ b^+, \quad db/d\tau = a^{+2}/2^{1/2}. \tag{1.2}$$

Here $\tau = \chi t$, where t is the interaction time.

The solution of the system of equations (1.2) in second-order perturbation theory in τ has the form

$$a = a_0 + 2^{1/2}\tau a_0^+ b_0^+ + \tau^2 (a_0^+ a_0 + 2b_0^+ b_0 + 2) a_0/2. \tag{1.3}$$

$$b = b_0 + \tau a_0^{+2}/2^{1/2} + \tau^2 (2a_0^+ a_0 + 1) b_0/2, \tag{1.4}$$

where the index "0" corresponds to the initial operators at $\tau = 0$. It is easy to verify that these solutions satisfy the standard commutation relations for bosons:

$$[a, a^+] = [b, b^+] = 1, \quad [a, b] = [a, b^+] = 0 \tag{1.5}$$

to second order in τ.

At the input of the parametric system we prescribe thermal noise with the average photon number

$$\langle a_0^+ a_0 \rangle = \langle b_0^+ b_0 \rangle = N_0.$$

Then the nonzero normally ordered operators of order S equal

$$\langle : (a_0^+ a_0)^S : \rangle = \langle : (b_0^+ b_0)^S : \rangle = S! N_0^S. \tag{1.6}$$

We employ the initial thermal noise mainly because this makes it possible to switch completely from the quantum model to the classical model. Indeed, the case $N_0 = 0$ corresponds to a vacuum at the input of the amplifier, i.e., a purely quantum situation. In the opposite limit $N_0 \gg 1$ the fact that the operators a_0, a_0^+ and b_0, b_0^+ do not commute no longer has any effect on the result and we arrive at the classical description of the system.

The transformation of the radiation by the interferometer (both the two-arm and polarization versions) in the course of the mixing of two modes in it is described by the following unitary transformation in the Heisenberg representation:[6,7]

$$a' = t^* a + r^* b, \quad b' = -ra + tb, \tag{1.7}$$

where the primes correspond to the output operators after mixing and t and r are the amplitude coupling coefficients of the interacting modes. In the simplest case of an interferometer in the form of only one beam splitter, t and r are the transmission and reflection coefficients. If, however, the interferometers shown in Fig. 1 are employed, then

$$T \equiv |t|^2 = \cos^2 \varphi, \quad R \equiv |r|^2 = \sin^2 \varphi, \tag{1.8}$$

where the corresponding intensity coefficients have been introduced and φ is one-half the relative phase delay in the Mach–Zehnder interferometer (Fig. 1a) or, in the polarization variant (Fig. 1b), the rotation angle of the polarization plane, introduced by the rotator (F).

For an output moment of order $2S = K + L$ successive applications of the transformation (1.7) give[6,7]

$$G'_{KL} = \sum_{p,\,q=0}^{2S} D^{(S)}_{Lp} D^{(S)*}_{Lq} \langle a^{+\tilde{p}} a^{\tilde{q}} b^{+p} b^{q} \rangle. \tag{1.9}$$

where

$$\tilde{p}=2S-p,\quad \tilde{q}=2S-q,$$

and $D^{(S)}_{Lp,q}$ are the matrix elements, of which we require

$$D_{10}^{(1)}=-tr^*,\quad L_{11}^{(1)}=T-R,\quad L_{12}^{(1)}=t^*r, \tag{1.10}$$

$$D_{10}^{(3/2)}=-t^2r^*,\quad D_{11}^{(3/2)}=t(T-2R),\quad D_{12}^{(3/2)}=r(2T-R),$$

$$D_{13}^{(3/2)}=t^*r^2, \tag{1.11}$$

$$D_{20}^{(2)}=t^2r^{*2},\quad D_{21}^{(2)}=2(R-T)tr^*,\quad D_{22}^{(2)}=T^2-4TR+R^2,$$

$$D_{23}^{(2)}=2(T-R)t^*r,\quad D_{24}^{(2)}=t^{*2}r^2. \tag{1.12}$$

Thus, using Eq. (1.6), we obtain

$$G_{11}'=TR(G_{02}+G_{20})+(T-R)^2G_{11}, \tag{1.13}$$

$$G_{21}'=T^2RG_{30}+T(T-2R)^2G_{21}+R(2T-R)^2G_{12}+TR^2G_{03}, \tag{1.14}$$

$$G_{22}'=2T^2R^2G_{40}+8TR(R-T)^2G_{31}+(T^2-4TR+R^2)^2G_{22}. \tag{1.15}$$

The remaining input moments of second to fourth orders with the initial thermal noise are equal to zero. In order to analyze the interference of three-photon states, we require only G_{21}'. We employ the other moments in the subsequent analysis.

According to Eqs. (1.3), (1.4), and (1.6) the required moments at the input of the interferometer equal

$$G_{30}\equiv\langle a^{+3}a^3\rangle=6N_0^3+18\tau^2(12N_0^4+15N_0^3+7N_0^2+N_0), \tag{1.16}$$

$$G_{21}\equiv\langle a^{+2}a^2b^+b\rangle=2N_0^3+2\tau^2(54N_0^4+78N_0^3+44N_0^2+11N_0+1), \tag{1.17}$$

$$G_{12}\equiv\langle a^+ab^{+2}b^2\rangle=2N_0^3+8\tau^2(9N_0^4+12N_0^3+6N_0^2+N_0), \tag{1.18}$$

$$G_{03}\equiv\langle b^{+3}b^3\rangle=6N_0^3+18\tau^2(3N_0^4+3N_0^3+N_0^2). \tag{1.19}$$

Substituting these expressions into Eq. (1.14) gives

$$\begin{aligned}G_{21}'=2N_0^3+(\tau^2/4)&\\ [225N_0^4+288N_0^3+140N_0^2+24N_0+1-x(9N_0^4&\\ +42N_0^3+46N_0^2+26N_0+5)&\\ +3x^2(45N_0^4+72N_0^3+44N_0^2+12N_0+1)&\\ +9x^3(9N_0^4+18N_0^3+14N_0^2+6N_0+1)].&\end{aligned} \tag{1.20}$$

Here

$$x=T-R=\cos 2\varphi.$$

In the purely quantum case, when a "squeezed" vacuum ($N_0=0$) exists at the input of the interferometer,

$$G_{21}'=\tau^2(1+x)(1-3x)^2/4. \tag{1.20}$$

It is interesting to compare this result with the case when the state at the input of the interferometer is described by the vector

$$|21\rangle\equiv|2\rangle_a|1\rangle_b, \tag{1.21}$$

i.e., two photons in the first mode and one photon in the second mode. In this case, the only nonzero moment at the input is $G_{21}=2$, and G_{21}' is identically equal to the moment (1.20) with $\tau=1$. Thus our Hamiltonian (1.1) indeed describes the process of preparation of two-mode three-photon states.

A plot of $G_{21}'/2$ as a function of φ, constructed in accordance with Eq. (1.20), is presented in Fig. 2. One can see that the moment G_{21}' has two zeros, and in addition the second zero corresponds to the absence of mixing in the channels ($T=0$, $R=1$), when the first mode is directed completely into the second channel and the second mode is directed completely into the first channel. The contrast of the interference pattern is thus equal to unity.

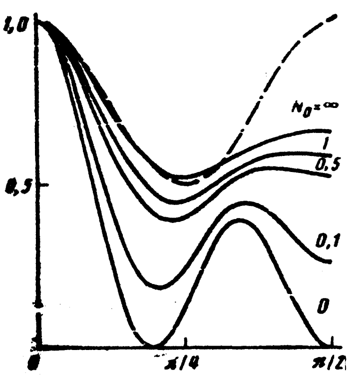

FIG. 2. Evolution of the interference curve $G_{21}'(\varphi)$ with a transition from the quantum ($N_0=0$) to the classical ($N_0\to\infty$) limit. The constant pedestal $2N_0^3$ is neglected. Normalization to the maximum value is performed everywhere. For comparison the dashed line illustrates the case of interference mixing of two independent identical coherent sources.

In the classical limit ($N_0\gg 1$) we have

$$G_{21}'=2N_0^3+{}^9/_4\tau^2N_0^4(25-x+15x^2+9x^3). \tag{1.22}$$

A normalized plot of the second interference term in Eq. (1.22) is also shown in Fig. 2. One can see that in this case a very faded interference pattern with quite low contrast is obtained. It is difficult to compare it with the "quantum" curve ($N_0=0$), but it is obvious that only significant smearing of the latter curve can result in such a metamorphosis. Thus the differences are qualitative. The reason for this is that the "quantum" moment G_{21}' is determined only by the nonzero input moment G_{21}', while in the classical description all four moments (1.16)–(1.19) play a role. As a result, significant "smoothing" of the interference minima occurs with increasing N_0; this is also illustrated by the plots in Fig. 2. Does this indicate pronounced qualitative differences between the classical and quantum models? Evidently yes, though only to the extent that the presence of interference is distinguished from virtually complete absence of interference. A distinct boundary between them is quite difficult to draw, in contrast to the four-photon states considered below.

It is interesting to compare these results with the case of interference mixing of two identical independent coherent modes. All input moments G_{30}, G_{21}, G_{12}, and G_{03} are equal to N_0^3, and

$$G_{21}'=N_0^3(1+x^2)/2. \tag{1.23}$$

The corresponding plot is also presented in Fig. 2 (dashed line). The symmetry in this case arises owing to the equivalence of the input modes; this is what distinguishes this case from interference mixing of thermal noise "squeezed" in the process of parametric amplification in both the classical and quantum approaches.

2. INTERFERENCE OF FOUR-PHOTON STATES

We now go up to the next step in the hierarchy of interference experiments: We pass from three- to four-photon states. In so doing, as before, we shall deal with two modes, which, however, are now symmetric: Two photons are generated in each mode at the input. Thus the schemes shown in Fig. 1 are transformed in an obvious manner: The channels for the passage of both modes will be identical. Correspondingly, detection must be performed with an even number of photodetectors. As before, total coincidence, i.e., appearance of photocounts in each of the detectors simultaneously, will constitute a positive result.

The fundamental possibilities of preparing four-photon states are the same as for three-photon states: multistage transitions of an atom from an excited state into the ground state accompanied by emission of four photons, parametric decay of the pump photon into two pairs in a medium with fourth-order nonlinearity $\chi^{(4)}$, and two-stage parametric scattering in piezoelectric crystals with quadratic nonlinearity, when nondegenerate parametric generation of two beams (signal and idler beams) occurs under intense monochromatic pumping and the two beams in turn pump a second stage, but this time a series of degenerate parametric converters. Thus a two-mode four-photon state is formed and enters the interferometer.

In the approximation of prescribed classical pumping, the process of formation of a four-photon state is described by the following Hamiltonian:

$$H_4=i\hbar\chi(a^{+2}b^{+2}-a^2b^2)/2, \qquad (2.1)$$

where the coefficient χ is proportional to $\chi^{(4)}$ (or $\chi^{(2)2}$ in the case of a two-cascade process) and to the pumping amplitude.

In the Heisenberg representation the evolution of the operators is determined by the following equations of motion:

$$da/d\tau=a^+b^{+2}, \quad db/d\tau=b^+a^{+2}. \qquad (2.2)$$

In second-order perturbation theory in τ we have

$$a=a_0+\tau a_0^+b_0^{+2}+\tau^2(2a_0^+a_0b_0^+b_0+a_0^+a_0+b_0^{+2}b_0^2 +4b_0^+b_0+2)a_0/2. \qquad (2.3)$$

An expression for b follows from Eq. (2.3) by interchanging a_0 and b_0. It can be verified directly that the commutation relations (1.5) are satisfied for terms of order no higher than quadratic in τ.

As previously, we assume that the noise at the input of the system is thermal. Under these conditions, we first analyze the possibility of observing interference of intensities accompanying mixing of the modes which are generated. This requires only two photodetectors.

The problem under consideration reduces to calculating the moment G'_{11}, which, according to Eq. (1.13), is determined by the input moments calculated with the help of Eqs. (1.6) and (2.3):

$$G_{20}\equiv\langle a^{+2}a^2\rangle=G_{02}\equiv\langle b^{+2}b^2\rangle =2[N_0^2+\tau^2(24N_0^4+40N_0^3+30N_0^2+10N_0+1)], \qquad (2.4)$$

$$G_{11}\equiv\langle a^+ab^+b\rangle=N_0^2+4\tau^2(12N_0^4+22N_0^3+18N_0^2+7N_0+1). \qquad (2.5)$$

Substituting these relations into Eq. (1.13) gives

$$G_{11}'=N_0^2+\tau^2[36N_0^4+64N_0^3+51N_0^2+19N_0+5/2 +(12N_0^4+24N_0^3+21N_0^2+9N_0+3/2)\cos 4\varphi]. \qquad (2.6)$$

In the purely quantum case, when a "squeezed" vacuum ($N_0=0$) exists at the input of the interferometer, we have

$$G_{11}'=5/2\,\tau^2(1+V\cos 4\varphi), \qquad (2.7)$$

where the visibility of the interference pattern is $V=3/5$.

We now compare this result with the case of the conversion of the state $|22\rangle=|2\rangle_a|2\rangle_b$. In this case, $G_{20}=G_{02}=G_{11}/2=2$ and G'_{11} is identical to Eq. (2.7) with $\tau=1$.

In the classical limit ($N_0\gg 1$)

$$G_{11}'=N_0^2+36\tau^2N_0^4[1+1/3\cos 4\varphi], \qquad (2.8)$$

i.e., the difference from the quantum case reduces only to a decrease in the visibility of interference: In Eq. (2.8) it is at most 1/3.

We recall that the moment G'_{11} describes standard intensity interferometry. We are mainly interested, however, in higher-order effects, in particular, the behavior of G'_{22}. In order to determine G'_{22}, we require moments, calculated with the help of Eqs. (1.6) and (2.3), of the form

$$G_{40}\equiv\langle a^{+4}a^4\rangle=G_{04}\equiv\langle b^{+4}b^4\rangle =24[N_0^4+\tau^2(80N_0^6+144N_0^5+116N_0^4+44N_0^3+6N_0^2)], \qquad (2.9)$$

$$G_{31}\equiv\langle a^{+3}a^3b^+b\rangle=G_{13}\equiv\langle a^+ab^{+3}b^3\rangle =6[N_0^4+\tau^2(224N_0^6+468N_0^5+446N_0^4+224N_0^3+57N_0^2+6N_0)], \qquad (2.10)$$

$$G_{22}\equiv\langle a^{+2}a^2b^{+2}b^2\rangle=4[N_0^4+\tau^2(288N_0^6+624N_0^5 +624N_0^4+330N_0^3+102N_0^2+16N_0+1)]. \qquad (2.11)$$

Substituting these relations into Eq. (1.15) gives

$$G_{22}'=4N_0^4+\tau^2[528N_0^6+1056N_0^5+972N_0^4 +462N_0^3+120N_0^2+16N_0 +1+6x^2(80N_0^6+168N_0^5+168N_0^4+74N_0^3+6N_0^2-4N_0-1) +9x^4(16N_0^6 +48N_0^5+68N_0^4+46N_0^3+28N_0^2+8N_0+1)]. \qquad (2.12)$$

For $N_0=0$ Eq. (2.12) becomes

$$G_{22}'=\tau^2(3x^2-1)^2. \qquad (2.13)$$

If the quantum state at the input of the interferometer is described by the vector $|22\rangle$, then the only nonzero moment $G_{22}=4$ and G'_{22} acquires the form (2.13) with $\tau=1$.

Thus in the purely quantum case G'_{22} vanishes twice as τ varies from unity to zero (see Fig. 3). This result confirms the more general result of Refs. 6 and 7 concerning the mix-

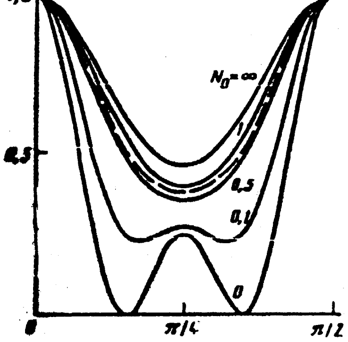

FIG. 3. Evolution of $G'_{22}(\varphi)$ with increasing N_0 for the case of the interference of two modes of a four-photon state. The pedestal $4N_0^4$ is neglected. The curves are normalized to the maximum value. For comparison the dashed line illustrates the case of interference mixing of two independent, identical, coherent sources.

ing of the two-mode ($2S$)-photon state: The moment G'_{SS} is proportional to the squared Legendre polynomial of order S, in particular,

$$G_{22}' \sim P_2^2(x).$$

The fact that the normalized moment $G'_{22}/G'_{22\,\max}$ oscillates in the full range from zero to unity (Fig. 3) indicates that the interference pattern can have a maximum possible contrast of unity, which, in general, is typical for the purely quantum case. Why then does the interference of intensities, according to Eq. (2.7), give a lower value of the contrast $V = 3/5$? The point is that G'_{11} consists of the linear superposition of two input moments G_{20} and G_{11}, and in addition both moments are different from zero. As a result some "smoothing" of the input minima, which is typical also of the classical description, occurs. On the other hand, the moment G'_{22} is determined only by the input moment G_{22}, and this is what gives the maximum possible contrast of the interference pattern. The general conclusion from this observation is this. In order to obtain the optimal contrast the number of photons of the quantum state $2S$ produced must be equal to the order $K + L$ of the recorded moment G'_{KL}.

We now analyze the classical limit $N_0 \gg 1$. In this case, according to Eq. (2.12), we have

$$G_{22}' = 4N_0^4 + 48\tau^2 N_0^6 (3x^4 + 10x^2 + 11). \qquad (2.14)$$

The normalized plot of the second interference term is also presented in Fig. 3. One can see that the two minima of the quantum case are replaced by a single, not so deep, dip of the classical case, and in addition it occurs in the region of the maximum of the first (quantum) case. Thus the differences become purely qualitative. The reason is still the same: In the classical description all input moments are nonzero.

We now compare this result with the case of interference mixing of two identical, independent, coherent modes. In this case

$$G_{40} = G_{31} = G_{22} = G_{13} = G_{04} = N_0^4$$

and

$$G_{22}' = N_0^4 (3 + 2x^2 + 3x^4)/8. \qquad (2.15)$$

The latter relation is identical to that obtained in Ref. 6. The corresponding plot, also presented in Fig. 3 (dashed line), exhibits an appreciable similarity with the case $N_0 \approx 1/2$ examined above.

CONCLUSIONS

The main result obtained in this work is that the transition from the two-photon to three- and four-photon interference experiments with mixing of a pair of prepared modes and detection of the moment of the corresponding order G'_{KL} ($K + L = 3$, 4; K and $L < 3$) introduces, aside from quantitative differences, significant qualitative differences also between the classical and quantum descriptions.

Thus each variant of interference considered above is interesting and possesses marked specificity.

[1]R. Ghosh and L. Mandel, Phys. Rev. Lett. **59**, 1903 (1987).
[2]Y. H. Shih, M. H. Rubin, and A. V. Sergienko, J. Sov. Laser. Res. **12**, 494 (1991); Phys. Rev. A (in press).
[3]J. G. Rarity and P. R. Tapster, Phys. Rev. A **45**, 2052 (1992).
[4]J. D. Franson, Phys. Rev. A **44**, 4552 (1991).
[5]J. Brendel, E. Mohler, and W. Martienssen, Phys. Rev. Lett. **66**, 1142 (1991).
[6]A. V. Belinsky and D. N. Klyshko, Laser Phys. **2**, 112 (1992).
[7]D. N. Klyshko, Phys. Lett. A **163**, 349 (1992).
[8]A. V. Belinsky and D. N. Klyshko, Phys. Lett. A 1992 (in press).
[9]D. M. Greenberger, M. Horne, A. Shimony, and A. Zeilinger, Am. J. Phys. **58**, 1131 (1990).
[10]M. Zukovski, Phys. Lett. A **157**, 203 (1991).
[11]J. Bell, Physics, N. Y. **1**, 195 (1964); J. F. Clauser and A. Shimony, Progr. Phys. **41**, 1881 (1978).
[12]C. Su and K. Wodkeiwich, Phys. Rev. A **44**, 6097 (1991).
[13]P. V. Elyutin and D. N. Klyshko, Phys. Lett. A **149**, 241 (1990).
[14]A. V. Belinskiĭ, Pis'ma Zh. Eksp. Teor. Fiz. **54**, 13 (1991) [JETP Lett. **54**, 11 (1991)].

Translated by M. E. Alferieff